

Coupling of Metabotropic Glutamate Receptor 8 to N-Type Ca^{2+} Channels in Rat Sympathetic Neurons

Juan Guo and Stephen R. Ikeda

Laboratory of Molecular Physiology, National Institute on Alcohol Abuse and Alcoholism, National Institutes of Health, Bethesda, Maryland

Received January 6, 2005; accepted March 8, 2005

ABSTRACT

Group III metabotropic glutamate receptors (mGluRs; mGluR4, 6, 7, and 8) couple to the $\text{G}\alpha_{i/o}$ -containing G protein heterotrimers and act as autoreceptors to regulate glutamate release, probably by inhibiting voltage-gated Ca^{2+} channels. Although most mGluRs have been functionally expressed in a variety of systems, few studies have demonstrated robust coupling of mGluR8 to downstream effectors. We therefore tested whether activation of mGluR8 inhibited Ca^{2+} channels. Both L-glutamate (L-Glu) and L-2-amino-4-phosphonobutyric acid (L-AP4), a selective agonist for group III mGluRs, inhibited N-type Ca^{2+} current in rat superior cervical ganglion neurons previously injected with a cDNA encoding mGluR8a/b. L-AP4 was ~ 100 -fold more potent ($\text{IC}_{50} = 0.1 \mu\text{M}$) than L-Glu ($\sim 10 \mu\text{M}$), but it had efficacy similar to that of L-Glu ($\sim 50\%$ maximal inhibition).

The potency and efficacy of L-AP4 and L-Glu were similar for both splice variants. Agonist-induced inhibition was abolished by pretreatment with (*R,S*)- α -cyclopropyl-4-phosphonophenylglycine, a selective group III mGluR antagonist, and pertussis toxin. Deletion of either a calmodulin (CaM) binding motif in the C terminus or the entire C terminus of mGluR8 did not affect mGluR8-mediated response. Our studies indicate that both mGluR8a and 8b are capable of inhibiting N-type Ca^{2+} channel, suggesting a role as presynaptic autoreceptors to regulate neuronal excitability. The studies also imply that the potential CaM binding domain is not required for the mGluR8-mediated Ca^{2+} channel inhibition and the C terminus of mGluR8a is dispensable for receptor coupling to N-type Ca^{2+} channels.

As a major excitatory neurotransmitter, glutamate functions through ligand-gated ionotropic and G protein-coupled metabotropic receptors (mGluRs). Genes coding for eight mGluRs (denoted mGluR1–8) with different splice variants have been identified and classified into three groups based on sequence homology, pharmacology, and signaling pathways (Nakanishi, 1994; Pin and Duvoisin, 1995; Conn and Pin, 1997). Group I mGluRs (mGluR1 and 5) mainly couple to $\text{G}\alpha_{q/11}$ containing G protein heterotrimer to activate phospholipase C, but they also couple to other G protein families, including $\text{G}\alpha_s$ and $\text{G}\alpha_{i/o}$ -containing G proteins. Group II (mGluR2 and 3) and group III mGluRs (mGluR4, 6, 7, and 8) couple to $\text{G}\alpha_{i/o}$ containing G protein family to inhibit adenylyl cyclase. With the exception of mGluR6, which is postsynaptic and exclusively expressed in the retina, group III mGluRs primarily serve as presynaptic autoreceptors to mediate feed-

back inhibition at glutamatergic synapses. However, at some synapses these receptors may also be localized at postsynaptic sites (Bradley et al., 1996; Kinoshita et al., 1996; Shigemoto et al., 1997).

mGluR8 was the last cloned subtype among the known mGluRs (Duvoisin et al., 1995). Its mRNA has been detected in the olfactory bulb, thalamus, pontine gray, cerebral cortex, hippocampus, cerebellum, and retina (Duvoisin et al., 1995; Saugstad et al., 1997). The mGluR8 receptor protein has been found in the dentate gyrus (Shigemoto et al., 1997), olfactory bulb, and the olfactory tubercle (Kinoshita et al., 1996; Wada et al., 1998). Electrophysiological studies suggested that mGluR8 functions as a presynaptic autoreceptor to regulate glutamate release from the lateral perforant path terminals in the mouse dentate gyrus (Zhai et al., 2002). It is suggested that mGluR8, like other group III mGluRs, controls glutamate release by inhibiting voltage-gated Ca^{2+} channels. However, unlike mGluR4 and mGluR7, which have been functionally expressed in a variety of heterologous system, few studies have reconstituted the coupling of mGluR8

Article, publication date, and citation information can be found at <http://molpharm.aspetjournals.org>.
doi:10.1124/mol.105.010975.

ABBREVIATIONS: mGluR, metabotropic glutamate receptor; PTX, pertussis toxin; GIRK, G protein-coupled inwardly rectifying potassium channel; CaM, calmodulin; SCG, superior cervical ganglion; MEM, minimal essential medium; mmGluR, mouse mGluR; PCR, polymerase chain reaction; EGFP, enhanced green fluorescent protein; rmGluR, rat mGluR; HEK, human embryonic kidney; TEA-OH, tetraethylammonium hydroxide; L-Glu, L-glutamate; CPPG, (*R,S*)- α -cyclopropyl-4-phosphonophenylglycine; L-AP4, L-2-amino-4-phosphonobutyric acid; I-V, current-voltage.

to its downstream effectors. mGluR8 was originally cloned from a mouse retina cDNA library; however, the characterization of mGluR8 was hindered by the fact that mouse mGluR8 coupled very weakly to the inhibition of adenylyl cyclase, with a maximal inhibition of ~20% (Duvoisin et al., 1995). On the other hand, glutamate elicited pertussis toxin (PTX)-sensitive potassium currents in *Xenopus laevis* oocytes coexpressing rat mGluR8 and G protein-coupled inwardly rectifying potassium (GIRK) channels (Saugstad et al., 1997). Therefore, as a rationale for the involvement of mGluR8 in regulating glutamate release, it is important to first establish whether voltage-gated Ca^{2+} channels involved in presynaptic inhibition are modulated by mGluR8.

mGluR7 was the first group III mGluR found to be highly localized at presynaptic active zones of hippocampal neurons (Shigemoto et al., 1997). It was reported recently that G protein $\beta\gamma$ subunits and the Ca^{2+} sensor calmodulin (CaM) interact in a mutually exclusive way within the proximal region of the C-terminal tail of mGluR7 (O'Connor et al., 1999). Based on this finding, it was proposed that CaM binds to the C terminus of mGluR7 to promote the dissociation of $\text{G}\beta\gamma$ from the receptors, thereby making the "released" $\text{G}\beta\gamma$ available for inhibiting voltage-dependent Ca^{2+} channels (O'Connor et al., 1999). In support of this notion, CaM inhibitors were shown to block group III mGluR-mediated inhibition of glutamate release in primary hippocampal neurons. Furthermore, deletion of the CaM binding motif from mGluR7 was shown to abolish $\beta\gamma$ subunit mediated signaling (O'Connor et al., 1999; El Far et al., 2001). Because the CaM binding motif is also present within the first 25 amino acid of the mGluR8 C terminus (El Far et al., 2001), the CaM binding motif in the mGluR8 C-terminal tail might participate in Ca^{2+} channel inhibition.

Therefore, in our present study, we first examined whether N-type Ca^{2+} channels could be modulated by activating mGluR8. We then tested whether the CaM binding motif in the C terminus of mGluR8 was involved in the Ca^{2+} channel modulation. We found that mGluR8 significantly inhibited N-type Ca^{2+} channels. However, the CaM binding domain in the C terminus was not required for the mGluR8-mediated Ca^{2+} channel inhibition. Furthermore, we determined that the entire mGluR8a C terminus was not crucial for receptor membrane expression and G protein coupling.

Materials and Methods

Preparation of Dissociated Sympathetic Neurons. Sympathetic cervical ganglion (SCG) neurons from adult male Wistar rats (150–300 g) were enzymatically dissociated as described previously (Ikeda, 2004). In brief, rats were decapitated after anesthesia by CO_2 inhalation as approved by the Institutional Animal Care and Use Committee. Bilateral SCG were dissected and desheathed, cut into small pieces, and then transferred into 6 ml of modified Earle's balanced salt solution containing 0.7 mg/ml collagenase D (Roche Diagnostics, Indianapolis, IN), 0.3 mg/ml trypsin (Worthington Biochemicals, Freehold, NJ) and 0.05 mg/ml DNase I (Sigma-Aldrich, St. Louis, MO). After incubation for 1 h in a shaking water bath at 36°C under an atmosphere of 5% CO_2 , 95% O_2 , SCG fragments were shaken vigorously to release the neuronal somata. The dissociated neurons were washed twice, resuspended in minimal essential medium (MEM) containing 10% fetal calf sera and 1% penicillin-streptomycin, plated onto poly-L-lysine-coated tissue culture dishes (35 mm), and placed in an incubator (95% air and 5% CO_2 ; 100% humid-

ity) at 37°C. After cDNA injection, the neurons were incubated overnight at 37°C, and current recordings were performed the following day. As appropriate, neurons were incubated overnight with 500 ng/ml PTX (List Biological Laboratories Inc., Campbell, CA).

DNA Cloning. Mouse mGluR8a (denoted mmGluR8a) cDNAs were cloned from mouse whole brain cDNA (BD Biosciences Clontech, Palo Alto, CA) using standard PCR techniques. To generate a mmGluR8a-EGFP fusion construct, full-length mmGluR8a was amplified using two primers: forward 5'-GATCGATCCTCGAGCAC-CATGGTTTGTGAGGGAAAGCGCTCAACC TCT-3' containing a XhoI restriction site and reverse 5'-GATCCCCGGGATCCGATT-GAATGATTA CTGTAGCTGATGTA-3' containing a XmaI restriction site. The amplification was carried out using PfuUltra high-fidelity DNA polymerase (Stratagene, La Jolla, CA) according to the following protocol: 95°C for 30 s, 60°C for 30 s, and 72°C for 3 min (35 cycles). The PCR fragment was analyzed on a 1% agarose gel, subcloned into pCR-Blunt II-TOPO vector (Invitrogen, Carlsbad, CA), and sequenced (CEQ8000; Beckman Coulter, Fullerton, CA). The mmGluR8a full-length cDNA was then subcloned into the XhoI and XmaI sites of expression vector pEGFP-N1 (BD Biosciences Clontech). QuikChange mutagenesis (Stratagene) was used to generate wild-type mmGluR8a (i.e., non-EGFP fusion) by changing the first linker amino acid glycine (GGA) to a stop codon (TGA). Likewise, wild-type rat mGluR8b (rmGluR8b; GenBank accession numbers NM022202 and Y11153) cDNA was amplified from rat whole brain cDNA library (BD Biosciences Clontech) using two primers: forward 5'-GATCAAGCTTCACCATGGTATGCGAGGGAAAGCGATCAGCC-3' containing a HindIII site and reverse 5'-GATCTCTAGATTAGGAAGT-GCTCCCGCTCTTGACCATCGGAAA-3' containing a XbaI site. The PCR fragment was subcloned into the HindIII and XbaI site of the pcDNA3.1 vector (Invitrogen) and sequenced. Because the amino acid sequence of C terminus of mouse mGluR8a and that of rat mGluR8a is identical, rat mGluR8a (rmGluR8a; GenBank accession number NM022202) cDNA was generated using QuikChange mutagenesis (Stratagene) by replacing the C terminus of rmGluR8b with that of mmGluR8a. The clone was confirmed by sequencing. Constructs with different deletions of the C terminus of mmGluR8a were generated using QuikChange mutagenesis (Stratagene). The deletions were confirmed by sequencing.

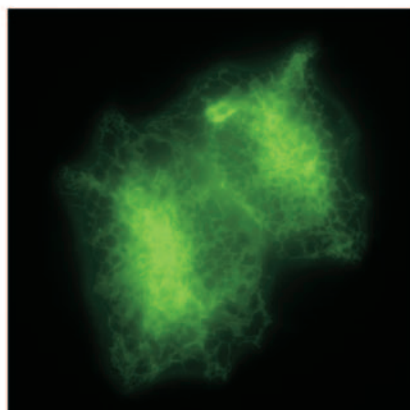
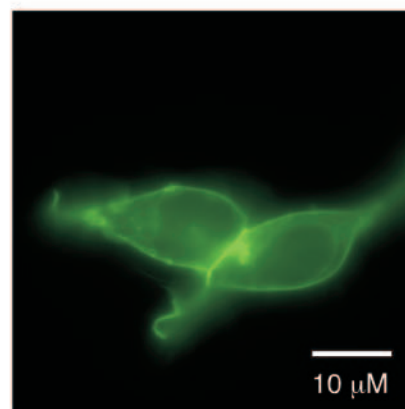
Cell Culture, Transfection, and Imaging. HEK293 cells were cultured in MEM supplemented with 10% fetal calf serum under an atmosphere containing 5% CO_2 . The cells were transfected with the mGluR8-EGFP cDNA as follows. A mixture of 1 μg of mGluR8-EGFP and 2 μl of LipofectAMINE 2000 (Invitrogen) was made in 100 μl of Opti-MEM and preincubated for 20 min. The mixture was then applied to cell culture wells containing HEK293 cells at ~95% confluence. After 24-h incubation, the cells were plated on glass-bottom chambers and examined using an Olympus IX-71 inverted fluorescence microscope equipped with a 60 \times 1.45 numerical aperture objective. Images were captured using a cooled charge-coupled device camera (Orca ERG; Hamamatsu, Hamamatsu City, Japan) and Openlab software (Improvision Inc., Lexington, MA).

cDNA Injection. As described previously (Ikeda, 2004; Ikeda and Jeong, 2004), microinjection of cDNA into neuronal nuclei was performed with an Eppendorf FemtoJet microjector and 5171 micromanipulator (Eppendorf, Madison, WI) using custom-designed software. Plasmids (pEGFP-N1, BD Biosciences Clontech; pcDNA3.1, Invitrogen) containing inserts coding for mmGluR8a, rmGluR8a, and rmGluR8b were stored at -20°C as 0.3 to 1 $\mu\text{g}/\mu\text{l}$ stock solution in TE buffer (10 mM Tris and 1 mM EDTA, pH 8). cDNA was injected at a pipette concentration of 100 to 200 ng/ μl . When EGFP-fusion constructs were not used, neurons were coinjected with EGFP cDNA (pEGFP-N1; 5 ng/ μl) to facilitate the identification of neurons receiving a successful intranuclear injection.

Electrophysiology. Rat SCG neurons were voltage clamped using the whole-cell patch-clamp technique with an Axopatch 200B amplifier (Axon Instruments Inc., Union City, CA). Electrodes were made from borosilicate glass capillaries (G85165T-4; Warner Instru-

A

mouse (AY673682)	1	MVCEGKRSTS	CPCFFLLTAK	FWILTMMQR	THSQEYAHSI	RLDGDIIILGG
mouse (U17252)		ST				L
rat (UM022202)		LA				V
	51	LFPVHAKGER	GVPCGDLKKE	KGIHRLEAML	YAIQINKDP	DLLSNITLGV
			D		T	
			E		I	
	101	RILDTCRDT	YALEQSLTFV	QALIEKDASD	VKCANGDPPI	FTKPKDKISGV
	151	IGAAASSVSI	MVANILRLFK	IPQISYASTA	PELSDNTRYD	FFSRVVPDSD
	201	YQAQAMVDIV	TALGWNVYST	LASEGNYGES	GVEAFTQISR	EIGGVVCIQAS
	251	QKIPREPRPG	EFEKIKRLL	ETPNARAVIM	FANEDDIRRI	LEAAKKNQSS
					G	
					R	
	301	GHFLWIGSDS	WGSKIAPVYQ	QEEIAEGAVT	ILPKRASIDG	FDRYFRSRTL
	351	ANNRRNVWFA	EFWEENFGCK	LGSHGKRNSH	IKKCTGLERI	ARDSSYEQEG
			S	S		
			W	E	L	
	401	KVQFVIDAVY	SMAYALHNMH	KELCPGYIGL	CPRMVTIDGK	ELLYIRAVN
				L		
				R		
	451	FNGSAGTPVT	FNENGDAPEG	YDIFQYQINN	KSTEYKIIGH	WTNQLHLKVE
	501	DMQWANREHT	HPASVCSLPC	KPGERKKTVK	GVPCWHCER	CEGYNYQVDE
					G	
					E	
	551	LSCELCPLDQ	RPNINRTGCQ	RIPIIKLEWH	SPWAVVPVFI	AILGIIATTF
					L	
					F	
	601	VIVTFVRYND	TPIVRASGRE	LSYVLLTGIF	LCYSITFLMI	AAPDTIICSF
	651	RRIFLGLGMC	FSYAALLTKT	NRIHRIFEQG	KKSVTAPKFI	SPASQLVITF
	701	SLISVQLLGV	FVWFVVDPPH	TIIDYGEQRT	LDPENARGVL	KCDISDLCLI
	751	CSLGYSILLM	VTCTVYAIKT	RGVPETFNEA	KPIGFTMYTT	CIIWLAFIPI
	801	FFGTAQSAEK	MYIQTTTLTV	SMSLSASVSL	GMLYMPKVYI	IIFHPEQNVO
	851	KRKRSFKAVV	TAATMQSKLI	QKGNDRPNGE	VKSELCESE	TNTSSTKTTY
	901	ISYSNHSI*				
		D				
		N				

B**C**

ment, Hamden, CT), coated with Sylgard (Dow Corning, Midland, MI), and fire polished to final resistances of ~ 2 M Ω when filled with internal solutions. Uncompensated series resistance was < 6 M Ω and generally electronically compensated $\sim 80\%$. Custom-designed software (S5) was used for voltage protocol generation and data acquisition on a Macintosh G4 computer (Apple Computer, Cupertino, CA) equipped with an ITC-18 data acquisition interface (InstruTECH Corporation, Port Washington, NY). Currents traces were filtered at 1 kHz (-3 dB) using a four-pole low-pass Bessel filter and digitized at 10 kHz with the 16-bit analog-to-digital converter in the ITC-18 data acquisition interface. All experiments were carried out at room temperature (22 – 26°C).

Solutions and Chemicals. For recording Ca^{2+} currents, the external solution consisted of 140 mM methanesulfonic acid, 145 mM tetraethylammonium hydroxide (TEA-OH), 10 mM HEPES, 10 mM glucose, 10 mM CaCl_2 , and 0.0003 mM tetrodotoxin, pH 7.4, with TEA-OH. The internal solution contained 120 mM *N*-methyl-D-glucamine, 20 mM TEA-OH, 11 mM EGTA, 10 mM HEPES, 10 mM sucrose, 1 mM CaCl_2 , 4 mM MgATP, 0.3 mM Na_2GTP , and 14 mM Tris-creatine phosphate, pH 7.2, with methanesulfonic acid. The osmolalities of the bath and pipette solutions were adjusted with sucrose to 325 and 300 mOsm/kg, respectively.

A gravity-driven perfusion system positioned ~ 100 μm from neurons was used for application of all drugs and control solutions. At the end of the perfusion system, a silica gas chromatography column was connected to six parallel columns of the same diameter in series. The column containing normal external solution was kept flowing to avoid flow-induced artifact until the desired solution was applied.

Stock solutions of L-glutamate (Sigma-Aldrich), L-2-amino-4-phosphonobutyric acid (L-AP4), and (*R,S*)-*R*-cyclopropyl-4-phosphonophenylglycine (CPPG; Tocris Cookson Inc., Ellisville, MO) were prepared in 100 mM NaOH at a stock concentration of 100, 1, and 10 mM, respectively. PTX (List Biological Laboratories Inc.) was prepared in H_2O at a stock concentration of 100 $\mu\text{g}/\text{ml}$. All drugs were diluted in the external solutions from stock solutions to the final concentrations just before use.

Data Analysis and Statistics. Currents were analyzed using Igor Pro software (WaveMetrics, Lake Oswego, OR) on an iMac computer. All data were expressed as mean \pm S.E.M. The Ca^{2+} current percentage inhibition (percentage) was determined as $(I_{\text{con}} - I_{\text{drug}})/I_{\text{con}} \times 100$, where I_{con} and I_{drug} are the Ca^{2+} currents before and after drug application. The concentration-response curves were fit to a Hill equation: $B = B_{\text{max}}/[1 + (\text{IC}_{50}/[\text{agonist}])^{n_H}]$, where B , B_{max} , IC_{50} , [agonist], and n_H are percentage of inhibition, maximum inhibition, half inhibition concentration, agonist concentration, and Hill coefficient, respectively. Statistical comparisons among groups were determined by analysis of variance. $P < 0.05$ was considered significant.

Results

Molecular Cloning of mmGluR8a. In preliminary studies, expression of the original mouse mGluR8a cDNA (GenBank accession no. U17252), a gift from Dr. R. Duvoisin (Oregon Health and Science University, Portland, OR), failed to couple to N-type Ca^{2+} channels in rat SCG neurons (data not shown), whereas expression of rat mGluR8b, an alternative splice variant that differs in the last 16 amino acids of the intracellular C terminus, robustly inhibited N-type Ca^{2+}

channels under the same conditions (this report). This finding seemed to indicate that residues in mGluR8 C terminus were important determinants of mGluR8 coupling to Ca^{2+} channels. We were surprised to find that exchanging the C termini of each clone failed to transfer the ability to modulate Ca^{2+} channels (data not shown). Rat mGluR8b was used in these studies because a cDNA sequence for the mouse ortholog was not available. Because the cognate residues of mouse and rat mGluR8 are highly conserved, it seemed unlikely that species differences could account for such profound differences in coupling. We thus undertook a detailed examination of the mouse mGluR8a clone (U17252) used in the preliminary studies. Comparing the mouse mGluR8a cDNA sequence U17252 with the mouse genome sequence using BLAT (Kent, 2002; <http://genome.ucsc.edu>) revealed eight potential amino acid differences in the translated sequence. Among these discrepancies, amino acid differences at position 343 and 589 probably arose from sequencing errors because our sequencing results at these positions (of the same clone) agreed with the genomic sequence. The remaining six amino acid differences seemed unlikely to result from legitimate polymorphisms because these residues are well conserved among rat, human, and mouse mGluR8 sequences. Because U17252 was the only full-length mouse mGluR8 cDNA sequence available in GenBank, we cloned mouse mGluR8 de novo from mouse brain cDNA. The newly cloned mouse mGluR8 was defined as mouse mGluR8a (mmGluR8a) because, like rat mGluR8a and -8b (rmGluR8a and rmGluR8b, respectively), an orthologous splice variant of mouse mGluR8b (mmGluR8b) is likely to exist (i.e., the alternatively spliced exon is present in the mouse genome).

Using primers based on a predicted mouse mGluR8a derived from mouse genomic sequence, a 2727-base pair PCR fragment was generated. Sequencing of the fragment revealed a 2727-base pair open reading frame, with original stop codon TGA replaced with GGA to generate an EGFP fusion construct. The mouse mGluR8a cDNA sequence predicts a protein of 908 amino acids with an estimated molecular mass of 101,820 Da. The mmGluR8a sequence (deposited in GenBank as accession no. AY673682) was 100% identical with the mouse genomic sequence located on chromosome 6. The deduced amino acid sequence of AY673682 revealed a 99.4 and 98.5% identity with rat and human orthologs, and 99.3% identity with the original mouse mGluR8. The differences between the mmGluR8a and the original mouse mGluR8 are depicted in Fig. 1A. The majority of the mutations (five amino acids) were located in the extracellular N terminus (the ligand-binding domain) of the receptor, and one mutation in the intracellular C terminus of the receptor. The two sequencing errors at positions 343 and 589 are indicated with boxes.

Expression of the original mouse mGluR8 fused to EGFP in HEK293 cells and hippocampal neurons revealed that the majority of the protein seemed trapped inside both HEK293

Fig. 1. Newly cloned mouse mGluR8a (AY673682) differs in sequence and expression pattern from U17252. A, alignment-predicted translation products from nucleotide sequence AY673682 with U17252 shows eight amino acid differences (red). The two residues affected by sequencing errors in U17252 are enclosed with boxes. The amino acid sequence of mouse mGluR8a (AY673682) shows a high identity with rat mGluR8a (NM022202); the differences are in blue. The putative signal sequence and the seven transmembrane domains are indicated with bars (Saugstad et al., 1997; Malherbe et al., 1999). B and C, expression of the EGFP-tagged constructs of U17252 (B) and AY67382 (C) in HEK293 cells shows different patterns of expression. Expression of the original mouse clone (U17252) revealed a lace-like pattern consistent with retention of protein in the endoplasmic reticulum. On the other hand, expression of AY673682 revealed a rim-like fluorescence pattern consistent with plasma membrane targeting.

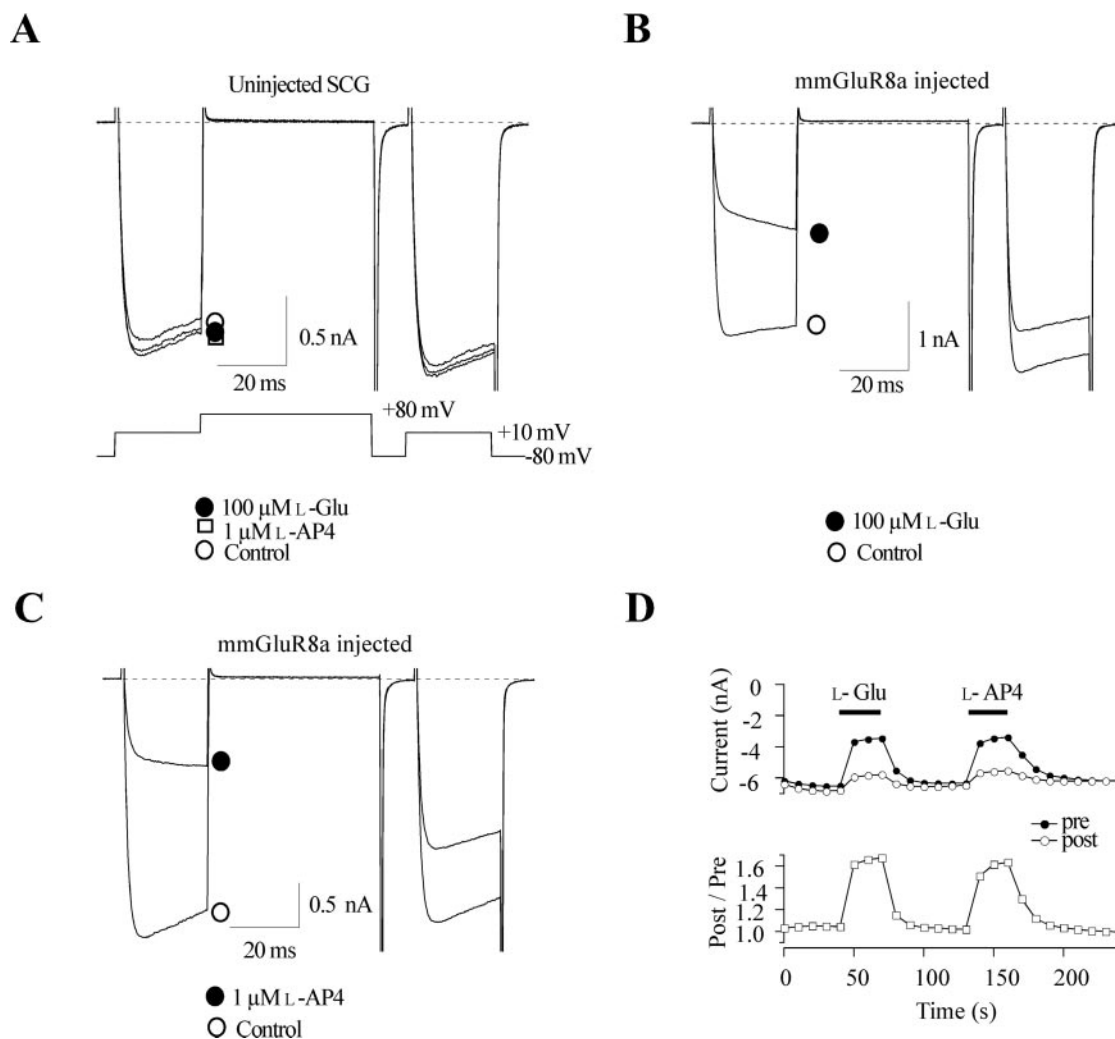


Fig. 2. Both L-Glu and L-AP4, a selective agonist for group III mGluRs, inhibit Ca^{2+} current in rat SCG neurons expressing mmGluR8a. A to C, superimposed Ca^{2+} current traces evoked with the double-pulse voltage protocol (bottom of A) in the absence and presence of 100 μM L-Glu and 1 μM L-AP4 from a control (A) and mmGluR8a expressing (B and C) neurons. Currents were evoked every 10 s. The dashed lines indicate the zero current level. D, time courses of the Ca^{2+} current amplitudes (top) and facilitation ratio (bottom) for a mmGluR8a-expressing neuron. Ca^{2+} current was measured 10 ms after initiation of the test pulse (+10 mV). Facilitation ratio (post/pre) was calculated as the ratio of Ca^{2+} current amplitude determined from the test pulse (+10 mV) occurring after (postpulse, \circ) and before (prepulse, \bullet) the +80-mV conditioning pulse. The closed bars indicate drug applications.

cells (Fig. 1B) and hippocampal neurons (data not shown). The fine lace-like pattern of fluorescence was consistent with retention in the endoplasmic reticulum. In contrast, expression of the newly cloned mouse mGluR8a-EGFP fusion construct displayed a rim-like fluorescence consistent with appropriate targeting of the protein to the plasma membrane (Fig. 1C). Therefore, the new mouse mGluR8a construct was used in all subsequent studies.

Functional Expression of mmGluR8a in Rat SCG Neurons. An important function of presynaptic group III mGluRs is to control glutamate release by inhibiting voltage-dependent Ca^{2+} channels via G protein $\beta\gamma$ subunits. Functional mGluRs are not endogenously expressed in rat SCG neurons (Ikeda et al., 1995); hence, this expression system facilitates the study of the coupling of molecularly defined mGluR subtypes to the effectors, such as Ca^{2+} channels (Kammermeier and Ikeda, 1999). We demonstrated previously that N-type Ca^{2+} channels are inhibited by activating a variety of mGluRs, including mGluR1, mGluR2, mGluR3, mGluR5, and mGluR7, heterologously expressed in rat SCG

neurons (Ikeda et al., 1995; Kammermeier and Ikeda, 1999, 2002). To test the function of the newly cloned mmGluR8a, we injected mmGluR8a cDNA into the nucleus of rat SCG neuron and tested whether the mmGluR8a inhibited Ca^{2+} channels. Figure 2 illustrates the effects of 100 μM L-Glu and 1 μM L-AP4, a selective agonist of group III mGluR, on Ca^{2+} channel currents elicited from uninjected and mmGluR8a cDNA-injected SCG neurons. Ca^{2+} channel currents were elicited every 10 s from a holding potential of -80 mV with a double-pulse protocol (Elmslie et al., 1990). This protocol consists of two identical 25-ms test pulses to +10 mV separated by a 50-ms strong depolarizing conditioning pulse to +80 mV (Fig. 2, A–C). The prepulse and postpulse currents were measured isochronally at 10 ms from the start of the test pulse. It has been demonstrated previously that the major component of Ca^{2+} current elicited from rat SCG neuron under these conditions is ω -conotoxin GVIA sensitive N-type Ca^{2+} current (Ikeda, 1991). Application of 100 μM L-Glu did not have an effect on Ca^{2+} current elicited from uninjected neurons (Fig. 2A), further indicating that func-

tional mGluRs are not expressed on the soma of rat SCG neurons (Ikeda et al., 1995; Kammermeier and Ikeda, 1999). For mmGluR8a cDNA-injected neurons, L-Glu (100 μ M) significantly inhibited the Ca^{2+} current by $51 \pm 4\%$ ($n = 11$). Figure 2B shows current traces elicited from a neuron previously injected with mmGluR8a cDNA in the absence or presence of 100 μ M L-Glu. As with many $\text{G}\alpha_{i/o}$ -containing G protein-coupled receptors, mmGluR8a inhibited Ca^{2+} current via a membrane-delimited, $\text{G}\beta\gamma$ -mediated voltage-dependent pathway characterized by slowed activation kinetics in the prepulse and partial relief of inhibition by a large depolarizing conditioning pulse (reviewed by Hille, 1994; Herlitze et al., 1996; Ikeda, 1996; Ikeda and Dunlap, 1999) (Fig. 2B). The ratio of postpulse current amplitude to prepulse current (post/pre), or facilitation ratio, was increased rapidly by mmGluR8a activation. Mean facilitation ratio increased from 1.06 ± 0.02 to 1.85 ± 0.11 ($n = 11$).

L-AP4 has been extensively used as a selective group III receptor agonist. As expected, 1 μ M L-AP4 produced the characteristic voltage-dependent Ca^{2+} channel inhibition (Fig. 2C) in mmGluR8a-expressing neurons. The mean Ca^{2+} current inhibition by 1 μ M L-AP4 was $54 \pm 2\%$ ($n = 18$). The facilitation ratio increased from 1.07 ± 0.03 to 1.90 ± 0.07 ($n = 18$). Both L-Glu- and L-AP4-induced Ca^{2+} current inhibition was rapid and reversible, reaching a steady-state level within ~ 10 s, and usually completely reversing within ~ 20 s upon washing the cell with control external solution (Fig. 2D).

The mmGluR8a-EGFP fusion construct was used in the majority of the present studies. To assess whether EGFP fusion affected mmGluR8a function, wild-type mmGluR8a cDNA was injected in the nucleus of rat SCG neuron. L-Glu (100 μ M) inhibited Ca^{2+} current by $52 \pm 5\%$ ($n = 4$) in the wild-type mmGluR8a-expressing neurons. The facilitation ratio increased from 1.09 ± 0.02 to 1.97 ± 0.14 ($n = 4$). There was no significant difference between the EGFP fusion and wild-type mmGluR8a-mediated Ca^{2+} channel inhibition ($P > 0.05$), suggesting that fusion of EGFP to the C terminus did not alter the coupling of mmGluR8a to N-type Ca^{2+} channels.

Rat mGluR8a has been shown to activate GIRK channels heterologously expressed in *Xenopus laevis* oocytes (Saugstad et al., 1997); however, the coupling of rat mGluR8a to the N-type Ca^{2+} channel has not been examined. Like mouse mGluR8a, activation of rat mGluR8a also produced voltage-dependent Ca^{2+} channel inhibition. L-Glu (100 μ M) inhibited Ca^{2+} current by $50 \pm 2\%$ ($n = 8$) in rmGluR8a-expressing neurons. There was no significant difference between mouse and rat mGluR8a-mediated Ca^{2+} channel inhibition ($P > 0.05$).

Inhibition of Ca^{2+} Currents by Activation of mGluR8b. The rat alternative splice variant rmGluR8b differs from rmGluR8a at the last 16 amino acids of the C terminus (Corti et al., 1998). Although mmGluR8b has not been cloned de novo, the alternatively spliced exon 9 responsible for rmGluR8b is found on mouse chromosome 6 and is very similar (98.0% identical) to the rat exon 9. Because the C terminus is important for coupling of some mGluRs, such as mGluR1 and mGluR7, we sought to examine whether mGluR8b modulated N-type Ca^{2+} current in mGluR8b-expressing neurons. As in mmGluR8a-expressing neurons, 100 μ M L-Glu and 1 μ M L-AP4 inhibited the Ca^{2+} current in all

the neurons injected with rat mGluR8b cDNA. Mean Ca^{2+} current inhibition in the presence of 100 μ M L-Glu and 1 μ M L-AP4 was $50 \pm 3\%$ ($n = 13$; Fig. 3A) and $53 \pm 2\%$ ($n = 13$; Fig. 3B), respectively. The Ca^{2+} channel inhibition was also voltage-dependent based on the slowing of current activation kinetics and the increased facilitation ratio. The facilitation ratio increased from 0.94 ± 0.02 to 1.59 ± 0.08 by L-Glu ($n = 13$) and from 1.01 ± 0.04 to 1.76 ± 0.09 by L-AP4 ($n = 13$).

Concentration-Dependent Ca^{2+} Current Inhibition by L-Glu and L-AP4 in mGluR8a/b-Expressing Neurons.

Fig. 4, A and B, show the time courses of concentration-dependent Ca^{2+} current inhibition induced by L-Glu and L-AP4 in two mmGluR8a-expressing SCG neurons. Because both L-Glu and L-AP4 induced Ca^{2+} current inhibition are rapid and reversible, a series concentrations of agonists were tested in a random order for each neuron. Figure 4C depicts the concentration-response curves of Ca^{2+} current inhibition in mmGluR8a- and rmGluR8b-expressing neurons. The data points represent the mean inhibition determined from four to 18 cells. For either L-Glu or L-AP4, at all concentrations tested, there was no significant difference between

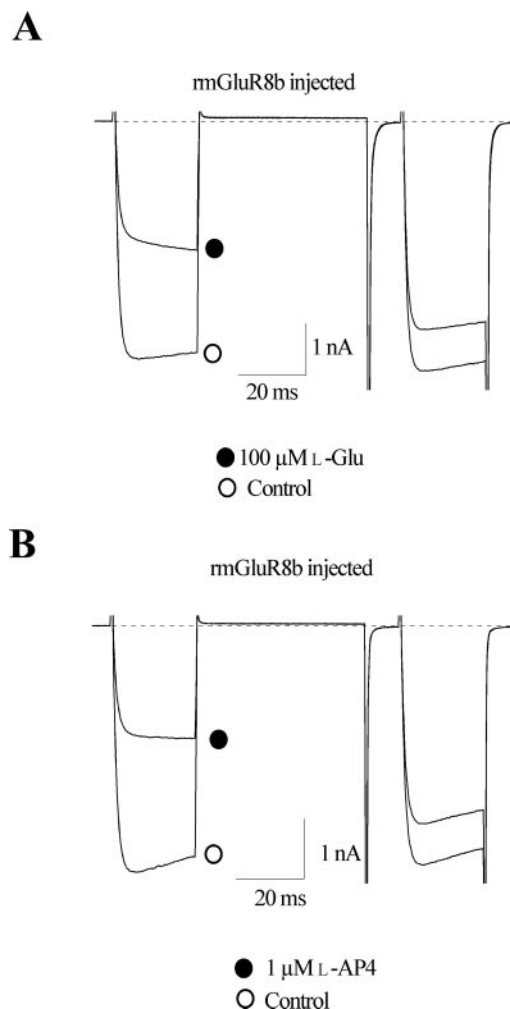


Fig. 3. Ca^{2+} current inhibition in SCG neurons expressing rat mGluR8b. A, superimposed Ca^{2+} current traces evoked from a neuron expressing rmGluR8b in the absence or presence of 100 μ M L-Glu. The dashed lines indicate the zero current level. B, superimposed Ca^{2+} current traces evoked from a neuron expressing rmGluR8b in the absence or presence of 1 μ M L-AP4. The dashed lines indicate the zero current. The measurement of Ca^{2+} current is illustrated in Fig. 1A.

mmGluR8a- and rmGluR8b-expressing neurons ($P > 0.05$). A Hill equation was fitted to the data using a nonlinear least-squares algorithm. From this analysis, the maximum inhibition, IC_{50} and Hill coefficient for L-Glu in mmGluR8a- and rmGluR8b-expressing neurons were 57 and 55%, 11 and 14

μM , and 0.9 and 0.8, respectively. For L-AP4, the maximum inhibition, IC_{50} and Hill coefficient were 62 and 62%, 0.1 and 0.1 μM , and 0.9 and 0.6, in mmGluR8a- and rmGluR8b-expressing neurons, respectively. Thus, L-AP4 was ~ 100 fold more potent than L-Glu, but it had a similar efficacy. The

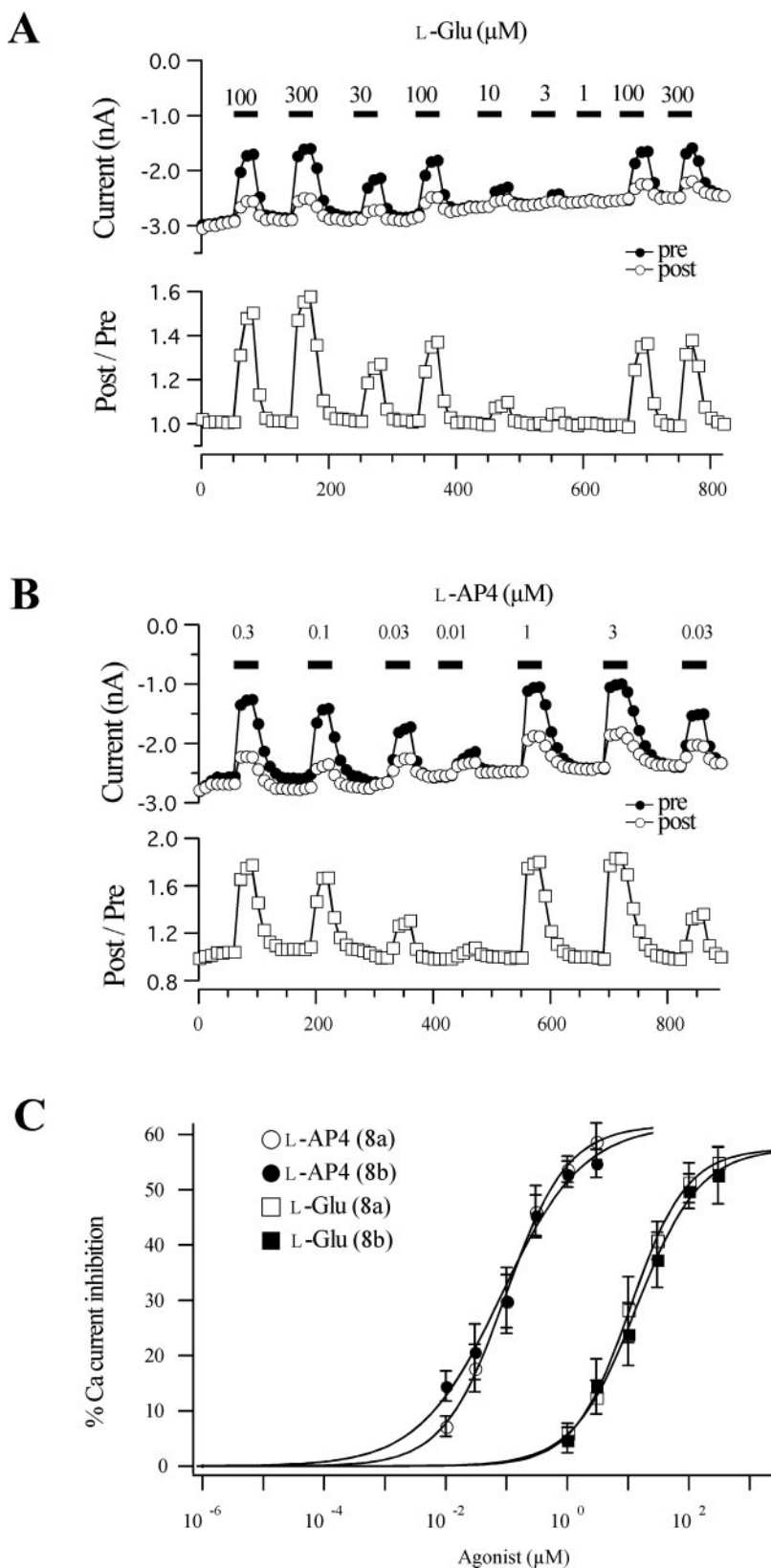


Fig. 4. Dose-dependent Ca^{2+} current inhibition in mmGluR8a- or rmGluR8b-expressing neurons. A and B, time courses of the Ca^{2+} current amplitudes (A and B, top) and facilitation ratio (A and B, bottom) for two mmGluR8a-expressing neurons. Ca^{2+} current was measured 10 ms after initiation of the test pulse (+10 mV). Facilitation ratio (post/pre) was calculated as the ratio of Ca^{2+} current amplitude determined from the test pulse (+10 mV) occurring after (postpulse, ○) and before (pre-pulse, ●) the +80-mV conditioning pulse. The filled bars indicate drug applications. C, smooth curves were obtained by fitting data to a Hill equation. Data are plotted as the mean \pm S.E.M. Each point on the dose-response curves represents the mean inhibition from four to 18 cells.

potency and efficacy of L-AP4 and L-Glu were similar for the two splice variants.

CPPG Prevented L-AP4-Induced Ca^{2+} Channel Inhibition in mmGluR8a/b-Expressing Neurons. CPPG is a selective group II/III mGluR antagonist. CPPG (300 μM) abolished L-Glu-activated GIRK currents in *Xenopus laevis* oocytes coinjected with rat mGluR8a and GIRK channels (Corti et al., 1998). To ascertain the pharmacological properties of the expressed receptors, CPPG was coapplied with 1 μM L-AP4. Figure 5, A and C, illustrates the L-AP4-induced Ca^{2+} current inhibition before and during coapplication of 1 μM CPPG in mmGluR8a- (Fig. 5A) and rmGluR8b (Fig. 5C)-expressing neurons. In all cells tested, 1 μM CPPG attenuated Ca^{2+} current inhibition in response to L-AP4 ($35 \pm 4\%$, $n = 9$; $18 \pm 4\%$, $n = 8$, for mmGluR8a and rmGluR8b, respectively), whereas 10 μM CPPG nearly abolished Ca^{2+} current inhibition ($6 \pm 1\%$, $n = 8$ for mmGluR8a; $1 \pm 1\%$, $n = 6$ for rmGluR8b). The effect of CPPG on L-AP4-induced Ca^{2+}

current inhibition was reversible because L-AP4 produced $\sim 50\%$ Ca^{2+} current inhibition after washout of the antagonist (Fig. 5B). Application of either 1 or 10 μM CPPG alone has no effect on Ca^{2+} current amplitude in mmGluR8a- and rmGluR8b-expressing neurons (Fig. 5, C and D).

Voltage-Dependent Inhibition by Activation of mmGluR8a and rmGluR8b Receptors. The effect of voltage on L-Glu- and L-AP4-induced Ca^{2+} current inhibition was characterized by generating current-voltage (I-V) relationships in the absence or presence of either 100 μM L-Glu or 1 μM L-AP4. Ca^{2+} currents were elicited from a holding potential of -80 mV with 70-ms test pulses between -120 and $+80$ mV. I-V curves (Fig. 6A) were normalized to the maximum Ca^{2+} current in the absence of agonist. The mean inhibition of Ca^{2+} currents produced by L-Glu and L-AP4 were plotted against membrane potential over the voltage range shown in Fig. 6B. L-Glu- and L-AP4-induced maximal inhibition at test potentials that generated the largest Ca^{2+} current (i.e.,

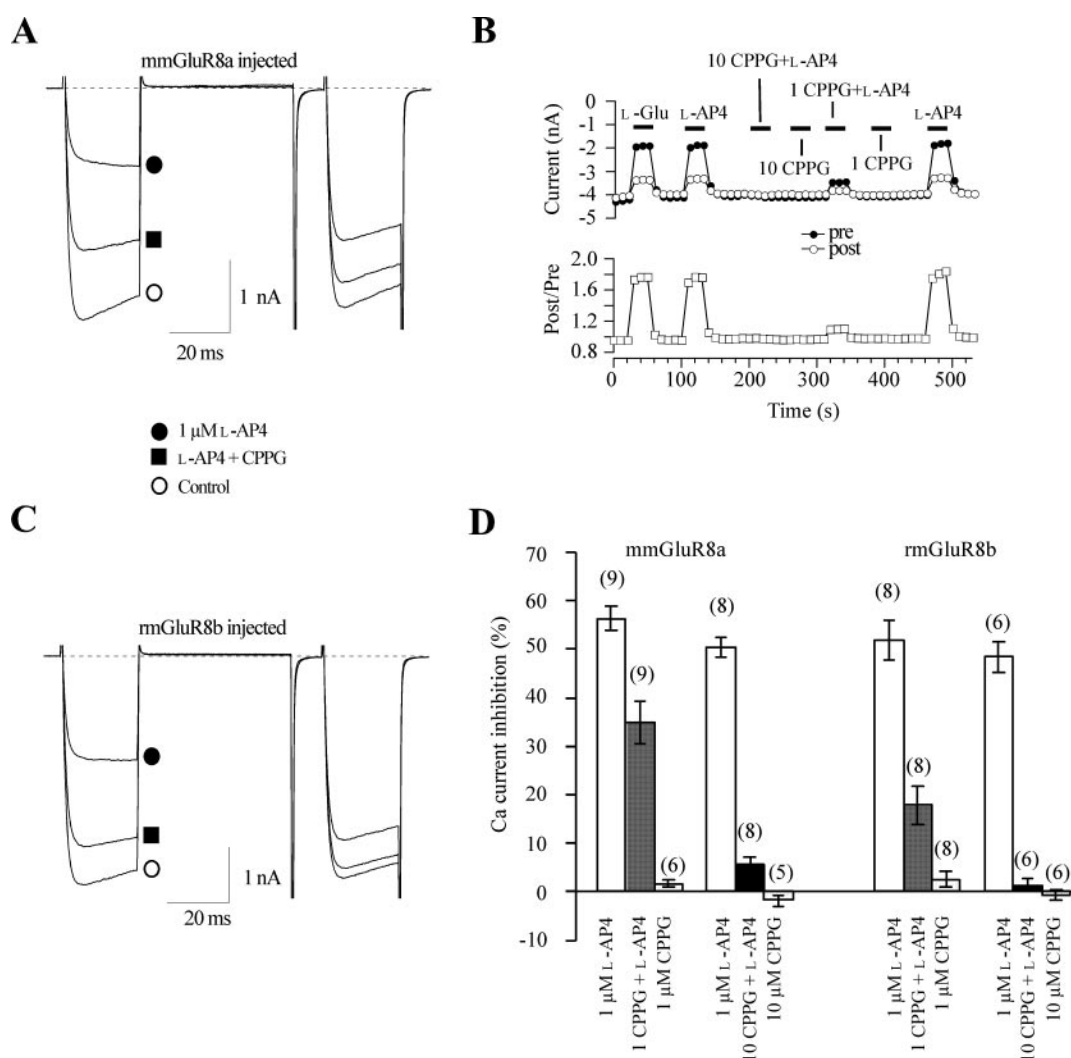


Fig. 5. CPPG, a selective group II/III mGluRs antagonist, significantly reduces Ca^{2+} channel inhibition mediated by mmGluR8a and rmGluR8b. A and C, superimposed Ca^{2+} current traces evoked from neurons expressing mmGluR8a (A) or rmGluR8b (C) in the absence or presence of 1 μM L-AP4, and in the presence of both 1 μM L-AP4 and 1 μM CPPG. B, time course of the Ca^{2+} current amplitudes (top) and facilitation ratio (bottom) for a mmGluR8a-expressing neuron. Ca^{2+} current was measured 10 ms after initiation of the test pulse ($+10$ mV). Facilitation ratio (post/pre) was calculated as the ratio of Ca^{2+} current amplitude determined from the test pulse ($+10$ mV) occurring after (postpulse, \circ) and before (prepulse, \bullet) the $+80$ -mV conditioning pulse. The solid bars indicate drug applications. D, summary graph of mean \pm S.E.M. Ca^{2+} current inhibition by 1 μM L-AP4, 1 μM L-AP4 + 1 μM CPPG, 1 μM L-AP4 + 10 μM CPPG, and 10 μM CPPG from neurons expressing mmGluR8a or rmGluR8b. Ca^{2+} current inhibition was measured isochronally 10 ms after initiation of the test pulse ($+10$ mV) in the absence or presence of drugs.

around 0 mV) in both mmGluR8a- and rmGluR8b-expressing neurons. The relationship between Ca^{2+} current inhibition and test pulse potentials displayed a “bell-shaped” profile, clearly indicating that the mGluR8a/b-mediated Ca^{2+} current inhibition was highly voltage-dependent.

PTX Blocked mGluR8a/b-Mediated Ca^{2+} Channel Inhibition. PTX is a useful tool for elucidating signaling pathways mediated by the $G_{i/o}$ protein. Group I mGluR inhibits Ca^{2+} channel via both $G_{i/o}$ - and $G_{q/11}$ -mediated pathways (Kammermeier and Ikeda, 1999). We therefore tested whether mGluR8-mediated Ca^{2+} inhibition involves a number of different G protein families as well. Unlike mGluR1, overnight pretreatment with 500 ng/ml PTX abolished the 100 μM glutamate-induced Ca^{2+} current inhibition in both mmGluR8a- and rmGluR8b-expressing neurons ($3 \pm 1\%$; $n = 5$; Fig. 7, A and C; and $4 \pm 1\%$; $n = 4$; Fig. 7, B and C, respectively), suggesting that only a PTX-sensitive G protein (i.e., a $G_{\alpha_{i/o}}$ -containing G protein) was involved in mGluR8-mediated Ca^{2+} current inhibition.

Deletion of the Intracellular C Terminus of mmGluR8a Did Not Affect Ca^{2+} Channel Modulation. It is well accepted that N-type Ca^{2+} channel modulation is mediated by G protein $\beta\gamma$ subunit released after activation of

G protein-coupled receptors. O'Connor et al. (1999) proposed a novel mechanism of presynaptic Ca^{2+} channel modulation in which the binding of CaM to the C terminus of group III mGluRs is required to release preassociated G protein $\beta\gamma$ subunits from the mGluRs. Thereafter, the dissociated $\beta\gamma$ subunits inhibit voltage-gated Ca^{2+} channels to control glutamate release. This model is supported by the fact that deletion of the CaM binding motif from mGluR7 and CaM antagonists prevents $\beta\gamma$ subunit-mediated modulation of GIRK channels by mGluR7. Because the same CaM binding motif was identified in the first 25 amino acid of the C terminus of mGluR8 (El Far et al., 2001), it was anticipated that the CaM binding motif in C terminus of mGluR8 might play a similar role in regulating Ca^{2+} channel activity. Therefore, we made a construct in which the first 26 amino acids (H844–L869) of the mmGluR8a C terminus were deleted (defined as mmGluR8a ΔC1 ; Fig. 8A). We were surprised to find that the deletion of the CaM binding motif did not affect glutamate-induced Ca^{2+} channel inhibition compared with the wild-type receptor ($P > 0.05$; Fig. 8C). Application of 100 μM L-Glu to neurons expressing mmGluR8a ΔC1 produced $51 \pm 5\%$ inhibition of Ca^{2+} current ($n = 9$), a value similar to wild-type receptors. Deletion of the

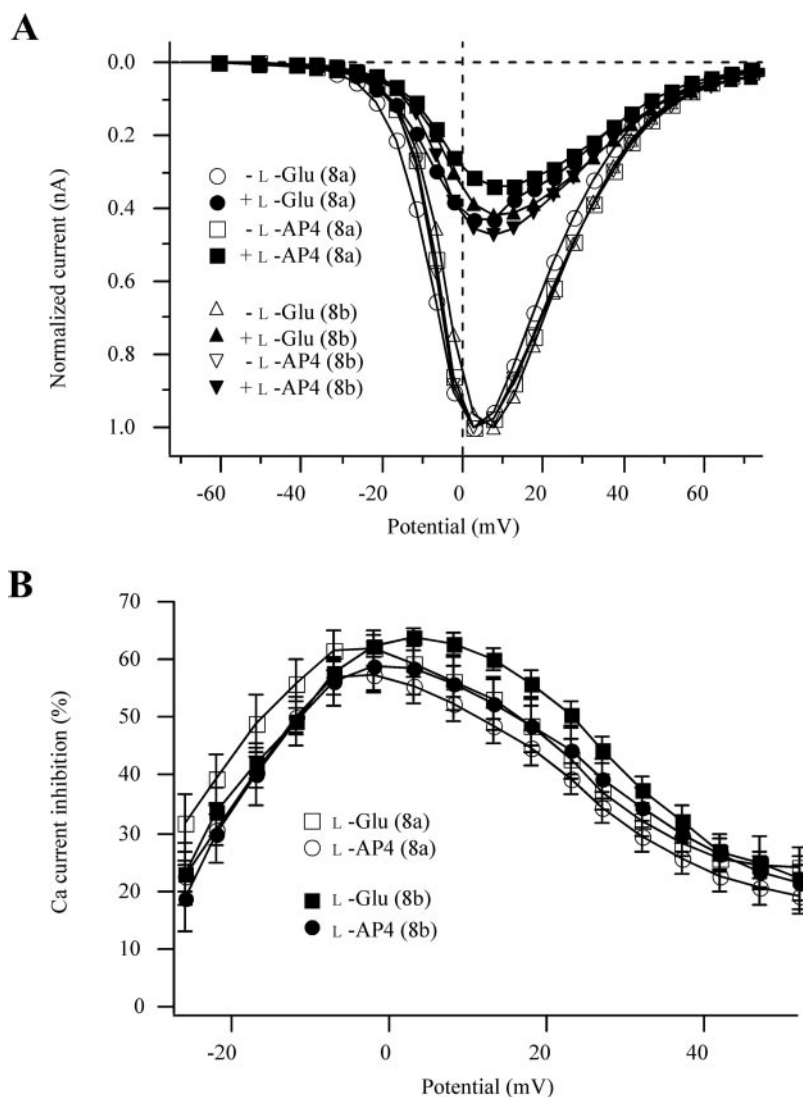


Fig. 6. Voltage-dependence of mGluR8a/b-mediated Ca^{2+} channel inhibition by L-Glu and L-AP4. **A**, normalized I-V relationship derived from currents of mmGluR8a- or rmGluR8b-expressing neurons in the absence or presence of 100 μM L-Glu or 1 μM L-AP4. Ca^{2+} currents were elicited with 70-ms voltage steps in 5- or 10-mV increments from -120 to $+80$ mV from a holding potential of -80 mV. The Ca^{2+} current at each voltage step was normalized to the Ca^{2+} current elicited by the depolarizing step to $+5$ mV in the absence of drugs. **B**, mean percentage of inhibition of Ca^{2+} currents was plotted against each voltage step to demonstrate the voltage-dependent Ca^{2+} channel inhibition by 100 μM L-Glu or 1 μM L-AP4.

middle 19 (I870–S888) (mmGluR8a Δ C2; Fig. 8A) and the last 20 amino acids (L889–I908) (mmGluR8a Δ C3; Fig. 8A) of the mmGluR8a C terminus also failed to impair the glutamate-induced Ca^{2+} channel inhibition. L-Glu (100 μM) blocked Ca^{2+} current by $47 \pm 8\%$ ($n = 4$) and $53 \pm 4\%$ ($n = 5$) in mmGluR8a Δ C2- and mmGluR8a Δ C3-expressing neurons, respectively (Fig. 8C). These data imply that the CaM binding domain in mGluR8 is not crucial for mGluR8-mediated Ca^{2+} channel modulation.

The mGluR7 C terminus has been shown to be necessary for cell surface delivery. Deletion of the mGluR7 C terminus produces a protein that is restricted to a perinuclear intracellular compartment, probably the Golgi and does not reach

the cell surface in hippocampal neurons (McCarthy et al., 2001). However, deletion of the entire mGluR8a C terminus (mmGluR8a Δ CT; Fig. 8A) did not affect mmGluR8a-mediated Ca^{2+} channel inhibition (Fig. 8B); 100 μM L-Glu inhibited Ca^{2+} current by $58 \pm 5\%$ ($n = 6$; Fig. 8C), which was not different from that produced by wild-type mmGluR8a ($P > 0.05$), suggesting that the mGluR8a C terminus is not crucial for the receptor membrane targeting and the coupling of the effectors.

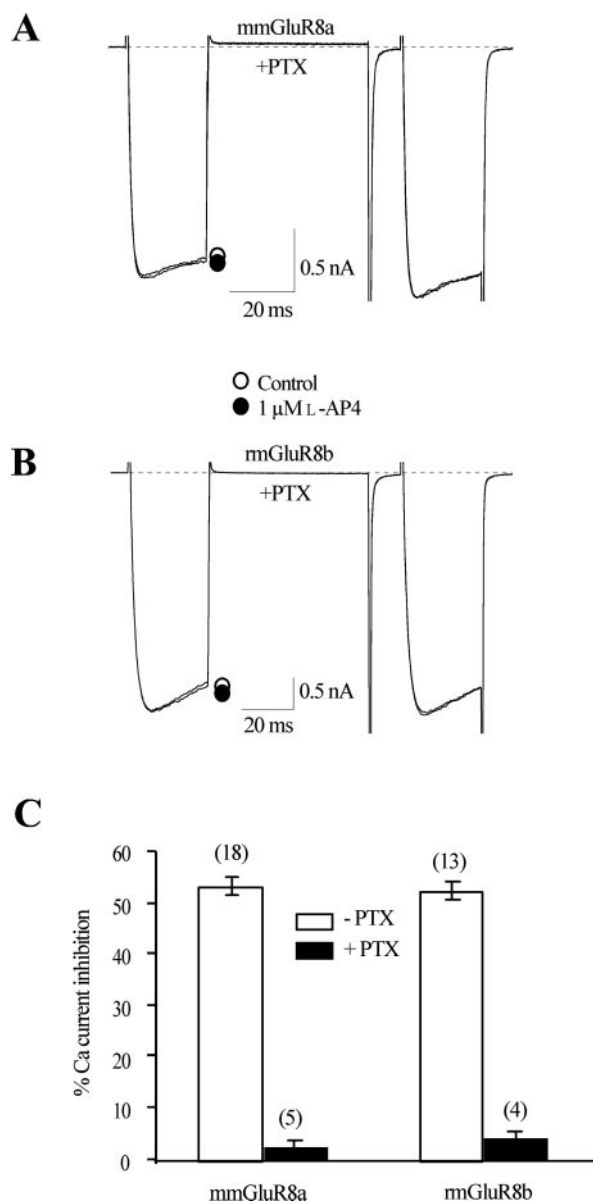


Fig. 7. PTX blocked mGluR8a/b-mediated Ca^{2+} current inhibition. A and B, superimposed Ca^{2+} current traces evoked from mmGluR8a- (A) or mmGluR8b (B)-expressing neurons pretreated with PTX in the absence or presence of 1 μM L-AP4. C, summary graph of mean \pm S.E.M. Ca^{2+} current inhibition by 1 μM L-AP4 from mGluR8a/b-expressing neurons with or without treatment of PTX. Ca^{2+} current inhibition was measured isochronally 10 ms after initiation of the test pulse (+10 mV) in the absence or presence of drugs.

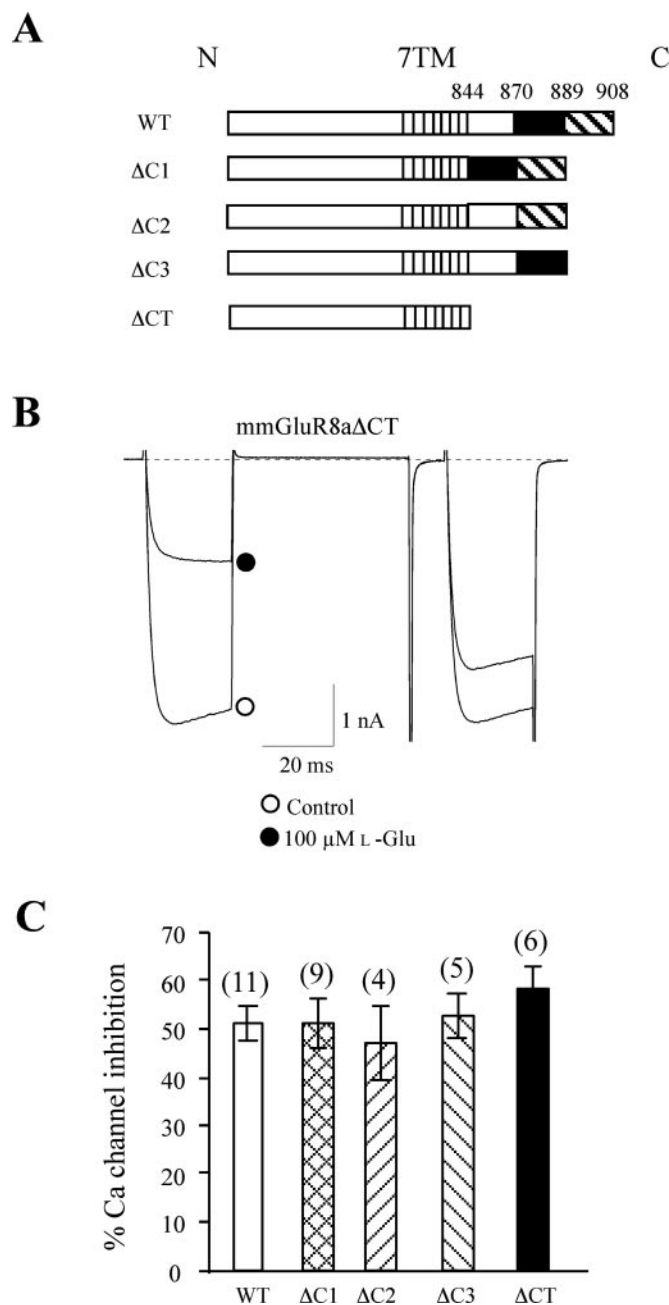


Fig. 8. Deletion of the intracellular C-terminal tail of mmGluR8a did not affect Ca^{2+} channel modulation. A, schematic illustrating the portions of the mmGluR8a C terminus deleted in different constructs as labeled. B, superimposed Ca^{2+} current traces evoked from a neuron expressing the mmGluR8a Δ CT construct in the absence or presence of 100 μM L-Glu. C, summary bar graph shows the 100 μM L-Glu induced Ca^{2+} channel inhibition for neurons injected with wild-type mmGluR8a, mmGluR8a Δ C1, mmGluR8a Δ C2, mmGluR8a Δ C3, or mmGluR8a Δ CT constructs. Ca^{2+} current inhibition was calculated as described in Fig. 2A. Numbers in parentheses indicate the number of neurons tested.

Discussion

All mGluR cDNA were originally cloned from rat, except for mGluR8, which was first cloned from a mouse retina cDNA library. The mouse cDNA clone encoding mGluR8a coupled weakly to the inhibition of adenylyl cyclase (Duvoisin et al., 1995) and failed to inhibit Ca^{2+} current in rat sympathetic neurons heterologously expressed with mouse mGluR8. However, heterologously expressed rat mGluR8a couples to GIRK channels in *X. laevis* oocytes (Saugstad et al., 1997) and N-type Ca^{2+} channel in rat sympathetic neurons (this report). The functional differences between rat and mouse mGluR8a are unlikely to have been caused by species variation because the two clones share 98.6% identity. Our experiments indicate that the original mouse mGluR8a lacks function because of inadequate trafficking of the receptor to the plasma membrane. It is likely that the amino acid discrepancies in the N-terminal domain in the original mouse mGluR8a account for the failure of mGluR8a delivery to the plasma membrane. The single amino acid discrepancy in the C terminus (N905D) cannot account for the receptor retention because a chimeric receptor, where the rmGluR8b C terminus was replaced by the C terminus of the original mouse mGluR8, is strongly plasma membrane targeted and couples to N-type Ca^{2+} channels (data not shown). The origins of the discrepancies found in the U17252 sequence are unclear although errors introduced by the PCR seem a likely possibility. The mmGluR8a cDNA sequence determined in this report (AY673682) has a 100% identity with putative exon genomic sequence, thus ruling out post-transcriptional modification.

Ca^{2+} channel inhibition is the proposed mechanism by which mGluR8 acts as autoreceptor to inhibit glutamate release. Like other group III mGluRs, mGluR8s are localized within presynaptic active zones and excluded from the soma of adult neurons. The inaccessibility of most presynaptic terminals to electrophysiological techniques makes it difficult to directly study the coupling of native mGluR8 to Ca^{2+} channels. Therefore, heterologous expression of mGluR8 by intranuclear injection of mGluR8 cDNA in an isolated adult mammalian neuron that has well studied G protein pathways facilitates in situ exploration of mGluR8. In this neuronal expression system, we demonstrated that activation of mouse mGluR8a and rat mGluR8b initiates a PTX-sensitive, voltage-dependent N-type Ca^{2+} channel inhibition.

Both group I and III mGluRs have splice variants that result from the use of alternative exons coding for different C termini (Conn and Pin, 1997). Although no functional differences between two variants of mGluR5 were reported (Minakami et al., 1994; Joly et al., 1995), functional differences between the variants of mGluR1 (mGluR1a and mGluR1b) were observed (Pin et al., 1992), suggesting that the long C-terminal domain of mGluR1a plays a role in receptor coupling efficiency. In our experiments, activation of either mGluR8a or mGluR8b produced a very similar Ca^{2+} channel inhibition, which is in agreement with the notion that the different C-terminal tails of the mGluR8 splice variants have minimal influence on G protein coupling efficacy (Corti et al., 1998).

L-AP4 is a potent group III receptor agonist. In *X. laevis* oocytes coexpressing rat mGluR8 and GIRK, both L-AP4 and L-Glu evoked inward potassium currents, where L-AP is ~4-

fold more potent than L-Glu (Saugstad et al., 1997). The EC_{50} values for L-AP4 and L-Glu were 0.67 and 2.5 μM , respectively (Saugstad et al., 1997). However, in our experiments, L-AP4 is ~100-fold more potent than L-Glu in mGluR8-mediated Ca^{2+} channel inhibition. IC_{50} values for L-AP4 and L-Glu are 0.1 and 11 μM , respectively. In studies of Saugstad et al. (1997), the Hill coefficient for L-AP4 and L-Glu was different, ~1 for L-AP4 and ~2 for L-Glu, whereas the Hill coefficients for L-AP4 and L-Glu were similar (~1) in the present study. The discrepancy between the two studies is not clear, but it may have been caused by differences in the expression conditions and channels studied.

We have demonstrated previously that group I mGluRs heterologously expressed in SCG neurons modulate both N-type Ca^{2+} and M-type K^{+} channels through discrete G protein signaling pathways (Kammermeier and Ikeda, 1999). Voltage-dependent Ca^{2+} channel inhibition occurred via a PTX-sensitive $\text{G}_{\alpha_{i/o}}$ -containing G protein. Voltage-independent Ca^{2+} channel inhibition and M-type K^{+} channel inhibition arise from a PTX- and CTX-insensitive G protein, presumably $\text{G}_{\alpha_{q/11}}$ -containing G protein. In the present study, PTX totally abolished Ca^{2+} channel inhibition, supporting the notion that mGluR8 couples to ion channels exclusively through the $\text{G}_{\alpha_{i/o}}$ class of heterotrimeric G proteins.

Several studies have shown that the C terminus in mGluR7a is involved in axon targeting and presynaptic clustering as well as binding CaM and $\text{G}\beta\gamma$ subunits. $\text{G}\beta\gamma$ and Ca^{2+} /CaM interact in a mutually exclusive way within the highly conserved first 25 amino acids of the C terminus of mGluR7. It is proposed that activated CaM displaces pre-bound $\text{G}\beta\gamma$ from mGluR7; the "released" $\text{G}\beta\gamma$ is then available for downstream signaling, such as inhibiting the N-type Ca^{2+} channel, thus inhibiting glutamate release. Because the CaM binding motif is found in the C termini of most group III mGluRs, including mGluR4a, 7a, 7b, 8a, and 8b (El Far et al., 2001), one should expect that deletion of this CaM binding motif would abolish mGluR8-mediated Ca^{2+} channel inhibition. Deletion of this conserved CaM binding motif in the C terminus of mGluR8a did not affect the glutamate-induced Ca^{2+} channel inhibition, which was not expected. Deletion of the middle 19 and the distal 20 amino acids of the C terminus had no effect on the mGluR8a-mediated Ca^{2+} channel inhibition. mGluR8 may use the second intracellular loop cooperating with the other intracellular domains to couple to its effectors, such as group I mGluRs do (Gomez et al., 1996). Because the homology of the middle and the distal portion of the C terminus of mGluR7 and mGluR8 is not very high compared with the proximal portion of the C terminus where CaM binding site is located, the two type receptors may use two different mechanism to fulfill their function. On the other hand, although CaM binding site in the mGluR7 C terminus is required for coupling of GIRK channels in HEK293 cells, the involvement of the mGluR7 CaM binding site in N-type Ca^{2+} channel modulation remains to be determined. Without the C terminus, mGluR7 is trapped in perinuclear compartment in cultured hippocampal neurons and cannot be delivered to the membrane (McCarthy et al., 2001); however, the C terminus of mGluR8a may not be necessary for plasma membrane targeting, at least in our mammalian neuronal expression system, because mGluR8a ΔCT still coupled to G proteins and induced Ca^{2+} channel inhibition. Further experiments to quantify the expression level of

mGluR8a with different deletions of C terminus will help determine the role of mGluR8a C terminus in the membrane trafficking.

In summary, our results show both mGluR8a and mGluR8b are capable of eliciting voltage-dependent, PTX-sensitive N-type Ca^{2+} channel inhibition, suggesting a role as autoreceptors in the presynaptic site to regulate neuronal excitability. Despite the differences in the C-terminal tails, mGluR8a and mGluR8b have very similar pharmacological profiles in terms of Ca^{2+} channel modulation. Finally, neither CaM binding domain in the C terminus nor the entire C terminus of mGluR8a is required for receptor coupling to N-type Ca^{2+} channels.

Acknowledgments

We thank Dr. Robert M. Duvoisin for original mGluR8a cDNA and Dr. Diomedes Logothetis for GIRK4(S143T) cDNA. We also thank Dr. Huanmian Chen for transfection of hippocampal neurons and Dr. Henry Puhl for useful discussion.

References

- Bradley SR, Levey AI, Hersch SM, and Conn PJ (1996) Immunocytochemical localization of group III metabotropic glutamate receptors in the hippocampus with subtype-specific antibodies. *J Neurosci* **16**:2044–2056.
- Conn PJ and Pin JP (1997) Pharmacology and functions of metabotropic glutamate receptors. *Annu Rev Pharmacol Toxicol* **37**:205–237.
- Corti C, Restituito S, Rimland JM, Brabet I, Corsi M, Pin JP, and Ferraguti F (1998) Cloning and characterization of alternative mRNA forms for the rat metabotropic glutamate receptors mGluR7 and mGluR8. *Eur J Neurosci* **10**:3629–3641.
- Duvoisin RM, Zhang C, and Ramonell K (1995) A novel metabotropic glutamate receptor expressed in the retina and olfactory bulb. *J Neurosci* **15**:3075–3083.
- El Far O, Boffill-Cardona E, Airas JM, O'Connor V, Boehm S, Freissmuth M, Nanoff C, and Betz H (2001) Mapping of calmodulin and $\text{G}\beta\gamma$ binding domains within the C-terminal region of the metabotropic glutamate receptor 7A. *J Biol Chem* **276**:30662–30669.
- Elmslie KS, Zhou W, and Jones SW (1990) LHRH and GTP- γ S modify calcium current activation in bullfrog sympathetic neurons. *Neuron* **5**:75–80.
- Gomez J, Joly C, Kuhn R, Knopfel T, Bockaert J, and Pin JP (1996) The second intracellular loop of metabotropic glutamate receptor 1 cooperates with the other intracellular domains to control coupling to G-proteins. *J Biol Chem* **271**:2199–2205.
- Herlitze S, Garcia DE, Mackie K, Hille B, Scheuer T, and Catterall WA (1996) Modulation of Ca^{2+} channels by G-protein $\beta\gamma$ subunits. *Nature (Lond)* **380**:258–262.
- Hille B (1994) Modulation of ion-channel function by G-protein-coupled receptors. *Trends Neurosci* **17**:531–536.
- Ikeda SR (1991) Double-pulse calcium channel current facilitation in adult rat sympathetic neurones. *J Physiol (Lond)* **439**:181–214.
- Ikeda SR (1996) Voltage-dependent modulation of N-type calcium channels by G-protein $\beta\gamma$ subunits. *Nature (Lond)* **380**:255–258.
- Ikeda SR (2004) Expression of G-protein signaling components in adult mammalian neurons by microinjection. *Methods Mol Biol* **259**:167–181.
- Ikeda SR and Dunlap K (1999) Voltage-dependent modulation of N-type calcium

channels: role of G protein subunits. *Adv Second Messenger Phosphoprotein Res* **33**:131–151.

- Ikeda SR and Jeong SW (2004) Use of RGS-insensitive $\text{G}\alpha$ subunits to study endogenous RGS protein action on G-protein modulation of N-type calcium channels in sympathetic neurons. *Methods Enzymol* **389**:170–189.
- Ikeda SR, Lovering DM, McCool BA, and Lewis DL (1995) Heterologous expression of metabotropic glutamate receptors in adult rat sympathetic neurons: subtype-specific coupling to ion channels. *Neuron* **14**:1029–1038.
- Joly C, Gomez J, Brabet I, Curry K, Bockaert J, and Pin JP (1995) Molecular, functional and pharmacological characterization of the metabotropic glutamate receptor type 5 splice variants: comparison with mGluR1. *J Neurosci* **15**:3970–3981.
- Kammermeier PJ and Ikeda SR (1999) Expression of RGS2 alters the coupling of metabotropic glutamate receptor 1a to M-type K^{+} and N-type Ca^{2+} channels. *Neuron* **22**:819–829.
- Kammermeier PJ and Ikeda SR (2002) Metabotropic glutamate receptor expression in the rat superior cervical ganglion. *Neurosci Lett* **330**:260–264.
- Kent WJ (2002) BLAT - The BLAST-like alignment tool. *Genome Res* **12**:656–664.
- Kinoshita A, Ohishi H, Neki A, Nomura S, Shigemoto R, Takada M, Nakanishi S, and Mizuno N (1996) Presynaptic localization of a metabotropic glutamate receptor, mGluR8, in the rhinencephalic areas: a light and electron microscope study in the rat. *Neurosci Lett* **207**:61–64.
- Malherbe P, Kratzeisen C, Lundstrom K, Richards JG, Faull RL, and Mutel V (1999) Cloning and functional expression of alternative spliced variants of the human metabotropic glutamate receptor 8. *Brain Res Mol Brain Res* **67**:201–210.
- McCarthy JB, Lim ST, Elkind NB, Trimmer JS, Duvoisin RM, Rodriguez-Boulant E, and Caplan MJ (2001) The C-terminal tail of the metabotropic glutamate receptor subtype 7 is necessary but not sufficient for cell surface delivery and polarized targeting in neurons and epithelia. *J Biol Chem* **276**:9133–9140.
- Minakami R, Katsuki F, Yamamoto T, Nakamura K, and Sugiyama H (1994) Molecular cloning and the functional expression of two isoforms of human metabotropic glutamate receptor subtype 5. *Biochem Biophys Res Commun* **199**:1136–1143.
- Nakanishi S (1994) Metabotropic glutamate receptors: synaptic transmission, modulation and plasticity. *Neuron* **13**:1031–1037.
- O'Connor V, El Far O, Boffill-Cardona E, Nanoff C, Freissmuth M, Karschin A, Airas JM, Betz H, and Boehm S (1999) Calmodulin dependence of presynaptic metabotropic glutamate receptor signaling. *Science (Wash DC)* **286**:1180–1184.
- Pin JP and Duvoisin R (1995) The metabotropic glutamate receptors: structure and functions. *Neuropharmacology* **34**:1–26.
- Pin JP, Waeber C, Prezeau L, Bockaert J, and Heinemann SF (1992) Alternative splicing generates metabotropic glutamate receptors inducing different patterns of calcium release in *Xenopus* oocytes. *Proc Natl Acad Sci USA* **89**:10331–10335.
- Saugstad JA, Kinzie JM, Shinohara MM, Segerson TP, and Westbrook GL (1997) Cloning and expression of rat metabotropic glutamate receptor 8 reveals a distinct pharmacological profile. *Mol Pharmacol* **51**:119–125.
- Shigemoto R, Kinoshita A, Wada E, Nomura S, Ohishi H, Takada M, Flor PJ, Neki A, Abe T, Nakanishi S, et al. (1997) Differential presynaptic localization of metabotropic glutamate receptor subtypes in the rat hippocampus. *J Neurosci* **17**:7503–7522.
- Wada E, Shigemoto R, Kinoshita A, Ohishi H, and Mizuno N (1998) Metabotropic glutamate receptor subtypes in axon terminals of projection fibers from the main and accessory olfactory bulbs: a light and electron microscopic immunohistochemical study in the rat. *J Comp Neurol* **393**:493–504.
- Zhai J, Tian MT, Wang Y, Yu JL, Koster A, Baez M, and Nisenbaum ES (2002) Modulation of lateral perforant path excitatory responses by metabotropic glutamate 8 (mGlu8) receptors. *Neuropharmacology* **43**:223–230.

Address correspondence to: Dr. Stephen R. Ikeda, Laboratory of Molecular Physiology, National Institute on Alcohol Abuse and Alcoholism, Room TS-06, 5625 Fishers Lane, Bethesda, MD 20892-8815. E-mail: siked@mail.nih.gov